



Title	Synergistic role of retinoic acid signaling and Gata3 during primitive choanae formation
Author(s)	Kurosaka, Hiroshi; Mushiake, Jin; Mithun, Saha et al.
Citation	
Version Type	A0
URL	<a href="https://hdl.handle.net/11094/79001">https://hdl.handle.net/11094/79001</a>
rights	
Note	

***Osaka University Knowledge Archive : OUKA***

<https://ir.library.osaka-u.ac.jp/>

Osaka University

1 **Synergistic role of retinoic acid signaling and Gata3 during primitive choanae formation**

2  
3 Hiroshi Kurosaka<sup>1\*</sup>, Jin Mushiake<sup>1</sup>, Saha Mithun<sup>1</sup>, Yanran Wu<sup>1</sup>, Qi Wang<sup>1</sup>, Masataka Kikuchi<sup>2</sup>,  
4 Akihiro Nakaya<sup>2,3</sup>, Sayuri Yamamoto<sup>1</sup>, Toshihiro Inubushi<sup>1</sup>, Satoshi Koga<sup>4</sup>, Lisa L. Sandell<sup>5</sup>, Paul  
5 Trainor<sup>6,7</sup>, Takashi Yamashiro<sup>1</sup>.

6  
7 1. Department of Orthodontics and Dentofacial Orthopedics, Graduate School of Dentistry,  
8 Osaka University

9 2. Department of Genome Informatics, Graduate School of Medicine, Osaka University

10 3. Laboratory of Genome Data Science Graduate School of Frontier Sciences, The University of  
11 Tokyo

12 4. Laboratory for Innate Immune Systems, RIKEN Center for Integrative Medical Sciences

13 5. Department of Oral Immunology and Infectious Diseases, University of Louisville School of  
14 Dentistry

15 6. Stowers Institute for Medical Research

16 7. Department of Anatomy and Cell Biology, University of Kansas School of Medicine

17  
18  
19  
20 Author for correspondence

21 Hiroshi Kurosaka, DDS, PhD

22 [kurosaka@dent.osaka-u.ac.jp](mailto:kurosaka@dent.osaka-u.ac.jp)

23 Associate Professor

24 Department of Orthodontics and Dentofacial Orthopedics, Graduate School of Dentistry, Osaka  
25 University

28 **Abstract**

29 Developmental defects of primitive choanae, an anatomical path to connect the embryonic nasal and  
30 oral cavity, result in disorders called choanal atresia, which are associated with many congenital  
31 diseases and require immediate clinical intervention after birth. Previous studies revealed that  
32 reduced retinoid signaling underlies the etiology of choanal atresia. In the present study, by using  
33 multiple mouse models which conditionally deleted *Rdh10* and *Gata3* during embryogenesis, we  
34 showed that *Gata3* expression is regulated by retinoid signaling during embryonic craniofacial  
35 development and plays crucial roles for development of the primitive choanae. Interestingly, *Gata3*  
36 loss of function is known to cause hypoparathyroidism, sensorineural deafness and renal disease  
37 (HDR) syndrome, which exhibits choanal atresia as one of the phenotypes in humans. Our model  
38 partially phenocopies HDR syndrome with choanal atresia, and is thus a useful tool for investigating  
39 the molecular and cellular mechanisms of HDR syndrome. We further uncovered critical synergy of  
40 *Gata3* and retinoid signaling during embryonic development, which will shed light on novel  
41 molecular and cellular etiology of congenital defects in primitive choanae formation.

42

43 **Introduction**

44 Craniofacial defects account for approximately 30% of all congenital anomalies, a rate largely due to  
45 the complexity of craniofacial development (1). Although the etiology and pathogenesis of cleft lip  
46 and/or palate are relatively well investigated (2), the developmental origins of many craniofacial  
47 anomalies are not well understood at either the molecular or cellular level. Choanal atresia (CA) is a  
48 craniofacial malformation characterized by a blocked nasal airway (3, 4). The incidence of CA is 1  
49 in 5000 live births, and in cases of bilateral CA can be lethal. Therefore CA typically requires  
50 immediate intervention (5). In spite of this clinical significance, the basic etiology and pathogenesis  
51 of CA remains elusive. Although theoretical mechanisms have been proposed to explain the basis of  
52 choanal atresia, very little basic research using animal models has been performed, and conclusive  
53 answers have not been provided (6). It is well known that CA can occur in concert with various  
54 genetic disorders such as CHARGE syndrome and Crouzon syndrome (3). This indicates that  
55 multiple genetic pathways may underlie the development of primitive choanae formation and  
56 furthermore that disruption of these signaling pathways could result in CA. However, our knowledge  
57 of the interplay among molecular pathways during primitive choanae development is still  
58 rudimentary. In past studies, reduced retinoic acid signaling was proven to result in defects in  
59 primitive choanae formation and choanal atresia (4, 7). We previously identified multiple genes  
60 which exhibit significantly altered spatiotemporal patterns of expression in embryos with reduced

61 retinoic acid signaling (4). For example, the transcription factor *Gata3*, was significantly  
62 downregulated. *Gata3* is normally expressed at high levels in the developing facial processes during  
63 primitive choanae development in the normal situation, and interestingly, *GATA3* mutation in  
64 humans are associated with hypoparathyroidism, sensorineural deafness and renal disease (HDR)  
65 syndrome, which can also include craniofacial anomalies, such as CA (8-10). Multiple studies have  
66 investigated the role of *Gata3* in the parathyroid (11), cochlea (12, 13) and nephron duct (14) in  
67 order to determine the cellular and molecular mechanism underlying the development of each  
68 phenotype in HDR syndrome. In contrast, the pathogenesis of CA in HDR syndrome remains  
69 unknown. Here we generated tamoxifen-inducible *Gata3* knockout mice (*Ert2Cre:Gata3<sup>fx/fx</sup>*) to  
70 elucidate the role of *Gata3* in craniofacial and primitive choanae development. We discovered that  
71 temporal excision of *Gata3* during embryonic frontonasal development resulted in reduced cell  
72 division of both epithelial and mesenchymal cells, which led to failure of the development of  
73 primitive choanae. We also uncovered a critical interaction between retinoid and *Gata3* function  
74 during craniofacial development, the disruption of which underlies the etiology of choanal atresia.

75

## 76 **Results**

### 77 **Reduced *Gata3* expression is associated with choanal atresia (CA) in *Ert2Cre:Gata3<sup>fx/fx</sup>***

#### 78 **embryos**

79 To discover signaling pathway(s) potentially involved in regulating primitive choanae formation, we  
80 analysed RNA-seq datasets we generated from the maxillary complex of E11.5 *Ert2Cre:Rdh10<sup>fx/fx</sup>*  
81 and control littermate embryos, which exhibit CA (4). Putative protein interactome analyses were  
82 performed using the genes whose expression was either significantly reduced (blue) or elevated  
83 (red), with known associated proteins (green) (Figure 1A and B). From this analysis we detected  
84 several networks or clusters which included *Gata3* and whose expression was significantly reduced  
85 in *Ert2Cre:Rdh10<sup>fx/fx</sup>* mice (Figure 1B). In parallel we also assessed the expression of *Gata3* in the  
86 frontonasal process of E11.5 embryos via *in situ* hybridization. While strong *Gata3* expression could  
87 be observed in the lambda-doid region in control E11.5 where the lateral nasal prominence (LNP),  
88 medial nasal prominence (MNP) and maxillary portion of the first pharyngeal arch (MXP), embryos,  
89 a substantial reduction was evident in E11.5 *Ert2Cre:Rdh10<sup>fx/fx</sup>* embryos (Figure 1C and D). These  
90 results identified retinoid signaling as a candidate regulator of *Gata3* expression in the developing  
91 lambda-doid region, which anatomically presages the developing primitive choanae.

92

### 93 **Expression pattern of *Gata3* mRNA and *RARE-LacZ* during primitive choanae formation**

94 To further assess the correlation between *Gata3* expression and retinoid signaling during primitive  
95 choanae development, we performed *in situ* hybridization for *Gata3* in parallel with *β galactosidase*  
96 staining of *RARE-LacZ* embryos, which report retinoid signaling activity throughout the early stages

97 during frontonasal development. Strong *Gata3* expression was detected in the lambdoidal region in  
98 E11.0 embryos (Figure 2A). Frontal sections of stained embryos revealed that *Gata3* was expressed  
99 in both the epithelium and mesenchyme of the developing medial nasal and lateral nasal process at  
100 the position where the medial and lateral nasal processes were fusing (Figure 2B and D, red  
101 arrowhead). *RARE-LacZ* activity was detected around the developing lambdoidal region at E11.0  
102 (Figure 2C), and frontal sections revealed an overlap of *RARE-LacZ* expression with *Gata3*  
103 expression at the junction where the medial and lateral nasal processes fuse (Figure 2B and D, red  
104 arrowhead). As development proceeded, the expression domain of *Gata3* became prominent  
105 specifically in the primitive choanae (Figure 2E, red arrowhead) and became restricted  
106 predominantly in the mesenchyme (Figure 2F). The expression of *RARE-LacZ* likewise became  
107 prominent around the primitive choanae at the E12.0 stage (Figure 2G) with intense retinoid  
108 signaling activity present in both the epithelium and mesenchyme (Figure 2H). The overlap in  
109 expression of *Gata3* and retinoid signaling around the primitive choanae (Figure 2F and H, red  
110 arrowhead), implying a synergistic role for these factors in regulating primitive choanae formation  
111 and development.

112

### 113 **Elimination of *Gata3* disrupts formation of primitive choanae**

114 To functionally test the global role of *Gata3* during primitive choanae formation, tamoxifen-

115 inducible *Gata3* knockout mice were produced by intercrossing *Gata3<sup>fx/fx</sup>* mice (15) with *Ert2Cre*  
116 mice to generate *Ert2Cre:Gata3<sup>fx/fx</sup>* mice (16). E9.5 tamoxifen treatment results in reduction but not  
117 elimination of intact *Gata3* in the developing choanae at E12.5 in *Ert2Cre:Gata3<sup>fx/fx</sup>* embryos, as  
118 shown by *in situ* hybridization using RNA oligo probe against exon 4 of *Gata3* (Figure 3A and B).  
119 Tamoxifen administration at E9.5 results in 31% of *Ert2Cre:Gata3<sup>fx/fx</sup>* embryos exhibiting either  
120 choanal atresia or choanal stenosis at E13.5 (Table 1). A further 34% were lethal at the same stage  
121 (Table 1). Some of the *Ert2Cre:Gata3<sup>fx/fx</sup>* embryos presented with agenesis of the primitive choanae,  
122 while control *Gata3<sup>fx/fx</sup>* littermates exhibited normal choanae development (Figure 3C-F). Frontal  
123 histological sections of *Ert2Cre:Gata3<sup>fx/fx</sup>* embryos also confirmed the nasal cavity was blocked  
124 (Figure 3G and H). These results strongly indicate that *Gata3* expression during embryonic  
125 craniofacial development is critical for primitive choanae development, and that *Gata3* loss-of-  
126 function results in defects in primitive choanae formation.

127

### 128 **Nasal cavity morphogenesis and shape are malformed in *Ert2Cre:Gata3<sup>fx/fx</sup>* embryos**

129 To further characterize malformation of the choanae and investigate the role of *Gata3* in nasal cavity  
130 formation, we generated three dimensional reconstructions of the volumetric shape of the nasal  
131 cavity in red and oral cavity in yellow. Micro CT scanning was therefore performed on both E13.5  
132 control *Gata3<sup>fx/fx</sup>* and *Ert2Cre:Gata3<sup>fx/fx</sup>* embryos to which tamoxifen was administered at E9.5. The



133 shape of the nasal cavity was continuous from the nostril through the end of the nasal cavity and  
134 showed clear connection to the oral cavity in the control *Gata3<sup>fx/fx</sup>* embryos (Figure 4A,B and C),  
135 whereas in mutant embryos, the nasal cavity was discontinuous and abnormally shaped and lacked  
136 the connection with the oral cavity (Figure 4D E and F). These results indicate that *Gata3* plays a  
137 critical role in primitive choanae formation as well as continuous nasal cavity development.

138

139 **Reduced cell proliferation and increased cell death underly the etiology of CA, CS and nasal**  
140 **cavity deformation in *Ert2Cre:Gata3<sup>fx/fx</sup>* mice**

141 We previously revealed that reduced cell proliferation is a primary cause of CA during craniofacial  
142 development (4). We therefore assessed the pattern of cell proliferation during primitive choanae  
143 development via phosphorylated histone H3 (PHH3) immunostaining of sections through the  
144 frontonasal process. In control E11.5 embryos, both the nasal epithelium and craniofacial  
145 mesenchyme contained PHH3-positive cells (Figure 5A and B). The number of PHH3-positive cells  
146 was significantly reduced in *Ert2Cre:Gata3<sup>fx/fx</sup>* embryos both in the epithelium and mesenchyme  
147 cells during nasal cavity development (Figure 5C-F). Moreover, the nasal epithelial cells were  
148 irregularly aligned at the position of invagination in *Ert2Cre:Gata3<sup>fx/fx</sup>* embryos (Figure 5D). In  
149 parallel with analyses of alterations in proliferation we also examined the frontonasal processes for  
150 the induction of cell death. TUNEL staining revealed an endogenously low level of cell death in the

151 frontonasal process of control embryos (Figure 5G and H). In contrast, a significant elevation in the  
152 level of cell death was detected in both the frontonasal epithelium and mesenchyme in  
153 *Ert2Cre:Gata3<sup>fx/fx</sup>* embryos (Figure 5I,J,K and L). These results indicate that *Gata3* regulates  
154 proliferation and cell survival which are crucial for normal primitive choanae and nasal cavity  
155 development. Interestingly, the overall spatiotemporal patterns of cell death and proliferation in  
156 *Ert2Cre:Gata3<sup>fx/fx</sup>* embryos closely resembled that in *Ert2Cre:Rdh10<sup>fx/fx</sup>* embryos (4). This further  
157 substantiates the notion that retinoid signaling and *Gata3* play central and perhaps synergistic roles  
158 in the development of the primitive choanae and nasal cavity.

159

#### 160 **Vitamin A deficient diet in dams results in early lethality of *Ert2Cre:Gata3<sup>fx/fx</sup>* embryos**

161 To test for synergy between retinoid signaling and *Gata3* function during embryogenesis, the  
162 pregnant dams of *Ert2Cre:Rdh10<sup>fx/fx</sup>* embryos were placed on a vitamin A deficient diet from before  
163 mating and subsequently administered tamoxifen at E9.5 and the embryos were collected at E13.0.  
164 We observed a significant elevation in the incidence of developmental malformations, including  
165 lethality, in the *Ert2Cre:Gata3<sup>fx/fx</sup>* embryos on a vitamin A deficient diet (Table 1). Most of the  
166 *Ert2Cre:Gata3<sup>fx/fx</sup>* embryos whose mothers consumed a vitamin A deficient diet for more than 20  
167 days showed signs of early lethality (no blood or heartbeat and opaque tissue, or resorption at E13.0)  
168 (Figure 6). Taken together, these results strongly suggest that retinoid signaling and *Gata3* function

169 act synergistically during embryogenesis to ensure embryo survival.

170

## 171 **Discussion**

### 172 **Investigation of critical factors associated with retinoid signaling during primitive choanae**

#### 173 **formation**

174 Multiple signaling pathways have been identified as key regulators of embryonic craniofacial

175 development and retinoid signaling is one of the best studied molecular pathways (17, 18).

176 Eliminating *Rdh10*, a rate-limiting enzyme in the synthesis of retinoic acid causes severe craniofacial

177 defects, including CA (4, 19, 20). Using a temporal conditional model of retinoid deficiency we

178 previously identified a critical role for *Rdh10* and retinoid signaling in formation of the primitive

179 choanae. (4). However, the molecular etiology of CA has not been fully elucidated and thus requires

180 further investigation. From protein interactome analyses using the results obtained from RNAseq of

181 *Rdh10* mutant and control embryo maxillary complexes (4), we discovered one network or cluster

182 which pivoted on *Gata3* and exhibited significantly reduced expression (Figure 1A and B). Previous

183 reports have shown that *Gata3* loss-of-function in mice results in early lethality around E11 with

184 severe defects including craniofacial anomalies (21, 22). In addition, *GATA3* mutations in human

185 result in hypoparathyroidism, sensorineural deafness and renal disease (HDR) syndrome, a

186 constellation of anomalies that also includes craniofacial defects such as CA (8, 23). The fact that

187 *Gata3* is strongly expressed around the developing frontonasal process in combination with its  
188 connection to human disease motivated us to investigate the role of *Gata3* in CA and its association  
189 with retinoid signaling (24). First, we confirmed a substantial reduction of *Gata3* expression around  
190 the developing primitive choana in E11.5 *Rdh10* mutant mouse embryos (Figure 1C and D). These  
191 results strongly suggest that retinoid signaling maybe responsible for activating *Gata3* in specific  
192 tissues during craniofacial development, especially around the primitive choana. Additionally, the  
193 spatiotemporal patterns of *Gata3* expression and *Rare-LacZ* reporter activity overlap during  
194 craniofacial development, especially around the frontonasal process. Notably, the ventral part of the  
195 developing nasal epithelium in the frontonasal process, a critical tissue for epithelial invagination  
196 and for forming oronasal membrane (3), co-expresses both *Gata3* and *Rare-LacZ* reporter (Figure  
197 2B and D, red arrowhead). The overlapping expression of *Gata3* and *Rare-LacZ* reporter activity in  
198 the craniofacial epithelium implies a synergistic role for these molecular pathways in the process of  
199 primitive choanae development.

200

### 201 **Disturbed expression of *Gata3* results in congenital defects including CA**

202 To evaluate the functional role of *Gata3*, we utilized tamoxifen-inducible knock out mice  
203 (*Ert2Cre;Gata3<sup>flx/flx</sup>*) in this study (16). Importantly, when tamoxifen was administered at E9.5, 31%  
204 (11/35) of the E13.5 *Ert2Cre;Gata3<sup>flx/flx</sup>* embryos exhibited CA or choanal stenosis (CS) which

205 exhibit narrower primitive choanae (Table 1, Figure 3C-H). These results clearly demonstrate an  
206 essential role of *Gata3* in primitive choanae development. Interestingly, the expression of mRNA  
207 containing *Gata3* exon 4, which is located between the loxP sites, was not completely eliminated  
208 around the developing choanae (Figure 3A and B). Additionally, 34% (12/35) of E13.5  
209 *Ert2Cre;Gata3<sup>fx/fx</sup>* embryos exhibited early lethality. *Gata3* null mice are embryonic lethal around  
210 E11.5 (21). These results indicate that *Ert2Cre;Gata3<sup>fx/fx</sup>* embryos retain some limited expression of  
211 *Gata3* which enables them to survive long enough to present with CA and CS at E13.5. The fact that  
212 the remaining 34% of *Ert2Cre;Gata3<sup>fx/fx</sup>* embryos did not show either CA or CS suggests that there is  
213 a threshold level of *Gata3* expression required for normal primitive choanae development, below the  
214 defects occur.

215

### 216 **The cytological role of *Gata3* in primitive choanae and nasal cavity development**

217 Nasal cavity development requires continuous epithelial invagination and branching morphogenesis  
218 (25). Multiple genes and their pathways, such as *Fgf* and retinoid signaling, are known to be  
219 involved in this process (4, 26). In the present study, we discovered severe nasal cavity deformation  
220 in *Ert2Cre;Gata3<sup>fx/fx</sup>* embryos (Figure 4). We also found a significant reduction of cell proliferation  
221 in both the epithelium and mesenchyme surrounding the developing nasal cavity (Figure 5A-F).  
222 Epithelial proliferation is one mechanism known to be critical for epithelial folding and branching

223 morphogenesis in various organs, such as the salivary glands and lungs (27). Interestingly, *Gata3* has  
224 been reported to play critical roles in ductal invasion during mammary gland development (28). In  
225 addition to alterations in proliferation significant elevation in cell death was also observed in  
226 *Ert2Cre;Gata3<sup>fx/fx</sup>* embryos, especially in the ventral portion of the nasal cavity in the frontonasal  
227 processes (Figure 5G-L). Interestingly, a lack of retinoid signaling also causes similar cellular and  
228 developmental defects resulting in CA (4). These findings strongly suggest that *Gata3* regulates cell  
229 proliferation and cell survival in the developing nasal cavity, and this dysregulation of balance leads  
230 to nasal cavity defects, including CA and CS.

231

### 232 **Synergistic effect of retinoid and *Gata3* signaling in embryonic development**

233 To evaluate the synergistic effects of *Gata3* and retinoid signaling during frontonasal and choanae  
234 development, we reduced the level of retinoid signaling in *Ert2Cre;Gata3<sup>fx/fx</sup>* embryos by  
235 administering vitamin A deficient food to pregnant dams. Interestingly, this experimental model  
236 resulted in an exaggerated malformation phenotype together with a significant increase in lethality  
237 (Table 1 and Figure 6). Interestingly, critical interactions between *Gata3* and retinoid signaling has  
238 been proposed for nephric duct insertion during kidney development (29). Our study however is the  
239 first report to show a critical interaction between *Gata3* and retinoid signaling during embryonic  
240 craniofacial development, especially in the etiology and pathogenesis of CA and CS. These insights

241 provide new knowledge about the contribution of *Gata3* to craniofacial development and advance  
242 our understanding of the molecular and cellular mechanisms underpinning CA and CS.

243

## 244 **Material and Methods**

### 245 **Animals**

246 Previously reported *Ert2Cre;Gata3<sup>flx/flx</sup>* male mice were mated with *Gata3<sup>flx/flx</sup>* female mice in  
247 order to get *Ert2Cre;Gata3<sup>flx/flx</sup>* embryos (15, 16). *Rdh10<sup>flx/flx</sup>* mice were derived from ES cells

248 generated through KOMP and maintained as previously described (4, 20). These mice are

249 equivalent to C57BL/6N-Rdh10<sup>tm1a(KOMP)Wtsi</sup>. *Cre-ER<sup>T2</sup>* (B6.129

250 Gt(ROSA)26Sortm1(cre/ERT2)Tyj/J, Jax stock #008463) from the Jackson Laboratory. For

251 embryonic staging, the morning of identification of the vaginal plug was defined as E0.5.

252 *Ert2Cre* and *Rare-LacZ* reporter mice were obtained from RIKEN BRC (STOCK Tg(RARE-

253 Hspa1b/lacZ)12Jrt). Vitamin A deficient diet was purchased from CLEA Japan.

254

### 255 **Protein interactome analysis**

256 Mouse protein interactome data was obtained from the iRefIndex database (30). After

257 interactions between the same genes (self-interactions) were removed, 46,512 interactions were

258 extracted. Among those interactions, 316 associations that interacted with the differentially  
259 expressed genes were visualized using Cytoscape software (31).

260

#### 261 **Administration of tamoxifen**

262 In order to excise *Gata3* from the developing embryos, 40 ug/g-body of tamoxifen which was  
263 dissolved in 90% corn oil and 10% ethanol solution was administered by intraperitoneal  
264 injection of pregnant *Gata3<sup>fx/fx</sup>* dams at E9.5.

265

#### 266 **Whole mount *in situ* hybridization**

267 Whole-mount *in situ* hybridization of mouse embryos was performed as previously described (32).  
268 A minimum of three embryos of each genotype were examined per probe.

269

#### 270 **$\beta$ -galactosidase staining**

271 Staining for  $\beta$ -galactosidase expression in *RARE-lacZ* reporter mice was performed by fixing the  
272 tissue in 2% formaldehyde and 0.8% glutaraldehyde solution for 30 min at 4°C followed by  
273 treatment with 1mg/ml X-gal (Promega, # V3941) solution for 2 hours at room temperature.



274

275 **Whole-mount nuclear fluorescent imaging**

276 For analyzing choanal structure, the maxilla of the embryos were fixed in 4% PFA overnight at  
277 4°C. Fixed tissue were washed several times in PBS and stained directly with DAPI (Dojindo)  
278 (1:1,000) in PBS overnight at 4°C and visualized with a Olympus SZX16 stereomicroscope (33).

279

280 **Micro-CT analysis for evaluating the shape of nasal cavity**

281 The head of E12.5 embryos were stained with 0.3% phosphotungstic acid / 70% ethanol solution  
282 overnight and scanned with an R\_mCT2 (Rigaku) with 10 um slice pitch. The shape of the nasal  
283 cavity was traced and the images were processed using ITK-SNAP (General Public License) for  
284 3D reconstruction.

285

286 **Immunohistochemistry**

287 Antibodies against phospho-Histone-H3 (PHH3) (#05806, 1:200, Millipore) and E-Cadherin  
288 (#3195, 1:200, Cell Signaling Technology) were used with appropriate secondary antibodies. Cell

289 death analysis was performed using the In Situ Cell Death Detection kit (Roche, #11684795910)  
290 following the manufacturer's instructions. The differences among the mean numbers of PHH3  
291 and TUNEL positive cells in the epithelium and mesenchyme between control and  
292 *Ert2Cre;Gata3<sup>fl/fl</sup>* embryos were evaluated by Student's two-tailed unpaired t-test.  $P < 0.05$   
293 indicated statistical significance.

294

#### 295 **Statistical analysis**

296 Two-proportion Z test was performed to evaluate the incidence of phenotypes (Table 1).  $P < 0.05$   
297 indicated statistical significance.

298

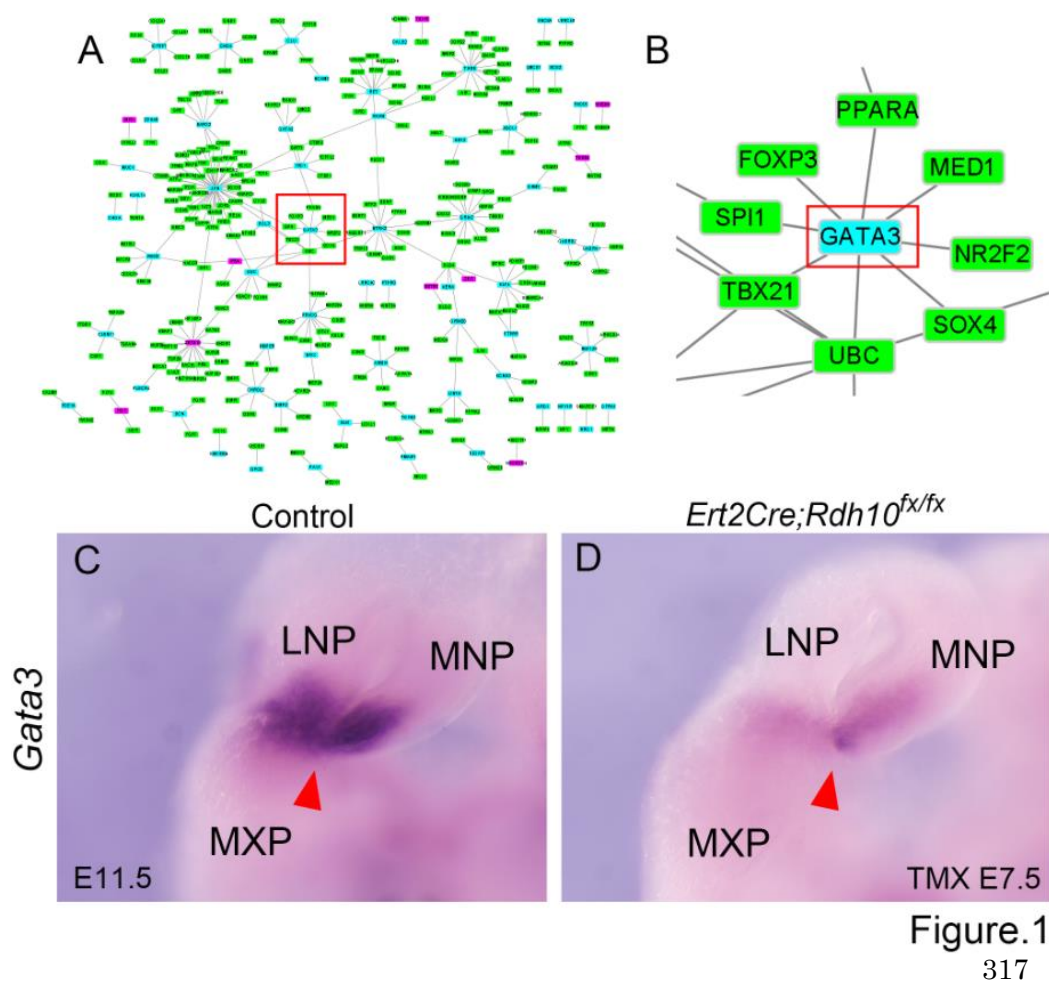
#### 299 **Acknowledgements**

300 The authors thank the members of the Department of Orthodontics and Orthopedics, Graduate School  
301 of Dentistry, Osaka University, for their insights and comments throughout the project. The authors  
302 also deeply appreciate Dr. Sachiko Iseki at Tokyo Medical Dental University, Dr. Kazuyo Moro  
303 at RIKEN IMS and Dr. Jinfang Zhu for providing the animal models used in this research. The  
304 work was supported by grants-in-aid for scientific research from the Japan Society for the Promotion

305 of Science (#16K15836, 15H05687 and 19H03858 to HK). Research in the Trainor lab is supported

306 by the Stowers Institute for Medical Research.

307



318 **Figure.1. Reduction of RA signaling results in reduced *Gata3* expression during craniofacial**  
 319 **development.** (A) The result of protein interactome analysis using the dataset of genes whose  
 320 expression had been previously shown by RNAseq to be altered by reduced retinoid signaling (4).  
 321 (B) A cluster pivoting *Gata3*. (C) RNA *in situ* hybridization of *Gata3* in the developing maxillary  
 322 complex. Strong *Gata3* expression could be detected in the lambdoidal region of the developing  
 323 maxillary complex (red arrowhead). (D) Substantial reduction of *Gata3* mRNA expression could be

324 observed in the retinoid deficient *ErtCre:Rdh10<sup>fl/fl</sup>* mutant to which tamoxifen was administered at

325 E7.5.

326

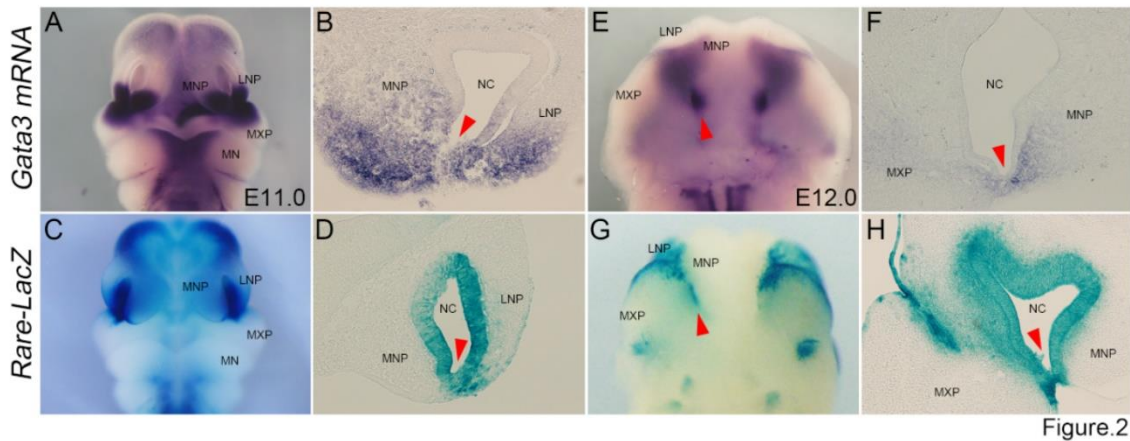


Figure.2.

327 **Figure 2. *Gata3* and retinoid signaling during frontonasal development. (A-F) *In situ***  
 328 hybridization of *Gata3* and (C-H)  $\beta$  galactosidase staining of the retinoid signaling reporter *Rare*  
 329 *LacZ* in developing head. Whole mount *in situ* hybridization for *Gata3* using embryonic head of  
 330 E11.0 in frontal view (A) and E12.0 in ventral view (E). Frontal section of E11.0 (B and D) and  
 331 E12.0 (F and H). Red arrowheads indicate the ventral epithelium of nasal cavity, which is important  
 332 for primitive choanae formation. MNP, medial nasal process. LNP, lateral nasal process. MXP,  
 333 maxillary process. NC, nasal cavity. MN, mandible.

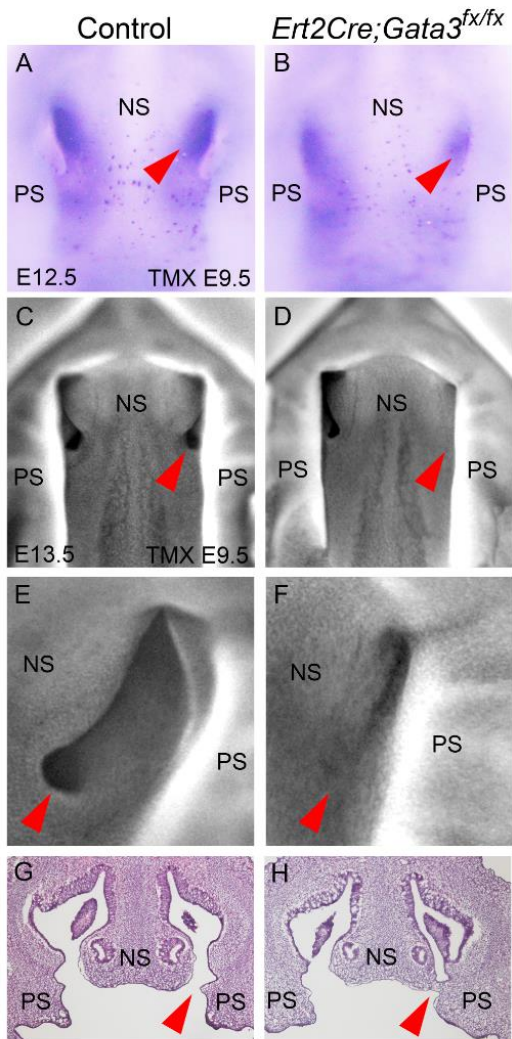


Figure.3.

334

335 **Figure 3. Temporal reduction of Gata3 expression result in defects in primitive choanae**

336 **development.** (A and B) *In situ* hybridization of exon 4 of *Gata3* at E12.5 in control (G) and

337 *Ert2Cre;Gata3<sup>fx/fx</sup>* (H) embryos. (C-F) Ventral view of developing choanae in E13.5 maxilla in

338 control (C and E) and *Ert2Cre;Gata3<sup>fx/fx</sup>* (D and F) embryos. (G and H) Hematoxylin and eosin

339 staining of frontal section of E13.5 heads in control (E) and *Ert2Cre;Gata3<sup>fx/fx</sup>* (F) embryos. Red

340 arrowheads indicate the position of developing choanae. TMX, tamoxifen treatment.

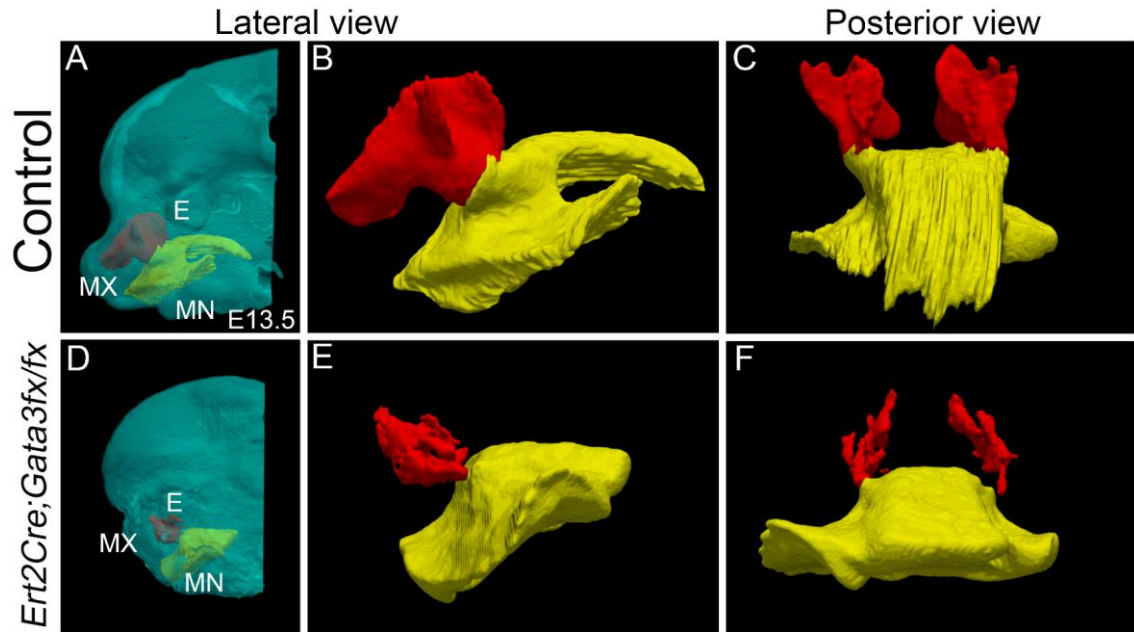


Figure.4

341

342 **Figure 4. Three-dimensional reconstruction of the shape of developing nasal and oral cavity. (A**

343 and D) Overlaid image of reconstructed head surface (light green), and nasal (red) and oral (yellow)

344 cavity seen from lateral view in E13.5 *Gata3<sup>flox/flox</sup>* control (A) and *Ert2Cre;Gata3<sup>flox/flox</sup>* (D) mouse to

345 which tamoxifen was administered at E9.5 (B, C, E and F). 3-dimensional reconstruction of the

346 shape of developing nasal (red) and oral (yellow) cavity in *Gata3<sup>flox/flox</sup>* control (B and C) and

347 *Ert2Cre;Gata3<sup>flox/flox</sup>* (E and F) embryo. E, eye. MX, maxilla. MN, mandible.

348



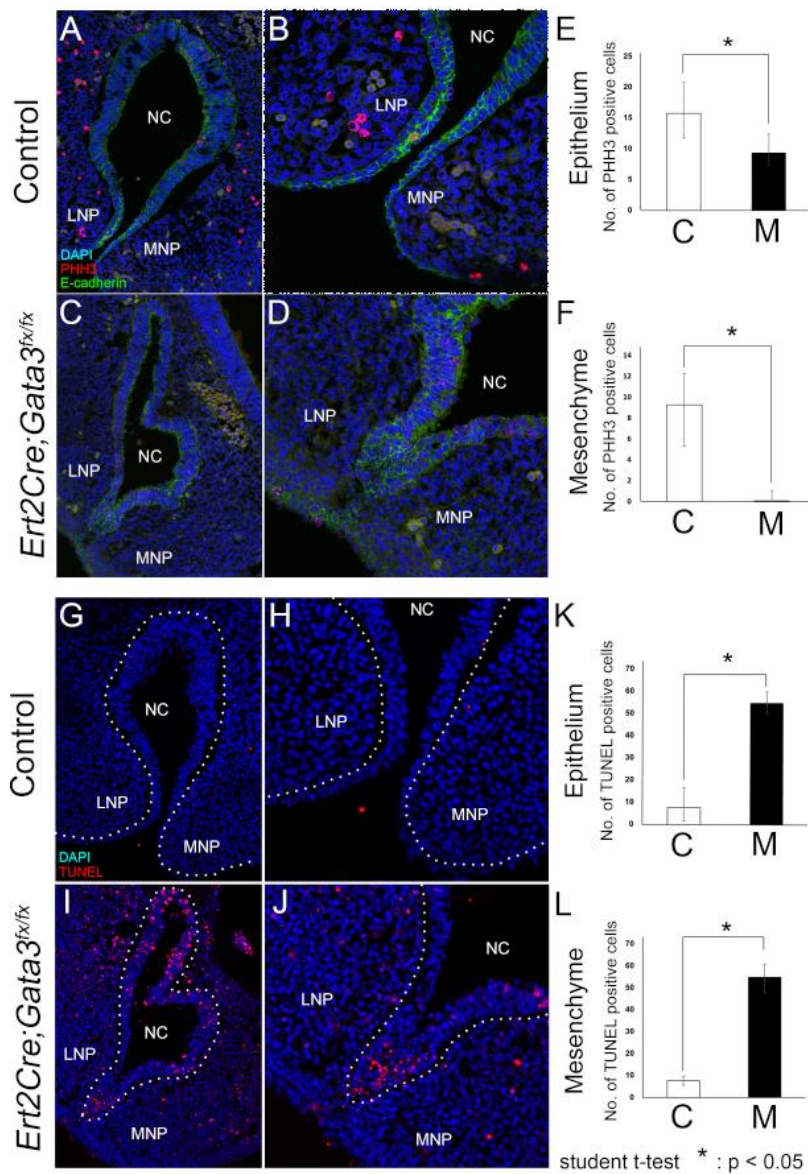


Figure.5.

362 **Figure 5. Cell proliferation and death in the process of development of primitive choana. (A-D)**

363 Immunohistochemistry of PHH3 (magenta) and E-CADHERIN (green) of frontal section of

364 developing nasal cavity in control (A and B) and *Ert2Cre;Gata3<sup>fx/fx</sup>* embryos (C and D). (G-J)

365 TUNEL staining to detect cell death (magenta) in developing nasal cavity in control (G and H) and

366 *Ert2Cre;Gata3<sup>fx/fx</sup>* (I and J) embryos. White dashed line indicates the boundary of nasal epithelium

367 and mesenchyme. B,D,H and J show magnified images of the ventral nasal cavity of A,C,G and  
368 I, respectively. Statistical analysis was performed using the number of PHH3- (E and F) and  
369 TUNEL-positive cells (K and L) in nasal epithelium and in the mesenchyme of nasal processes both  
370 in control (white bar) and *Ert2Cre;Gata3<sup>fx/fx</sup>* embryos (black bar). MNP, medial nasal process.  
371 LNP, lateral nasal process. NC, nasal cavity. C, control. M, mutant (*Ert2Cre;Gata3<sup>fx/fx</sup>*). Student T-  
372 test  $**P < 0.01$ .  
373

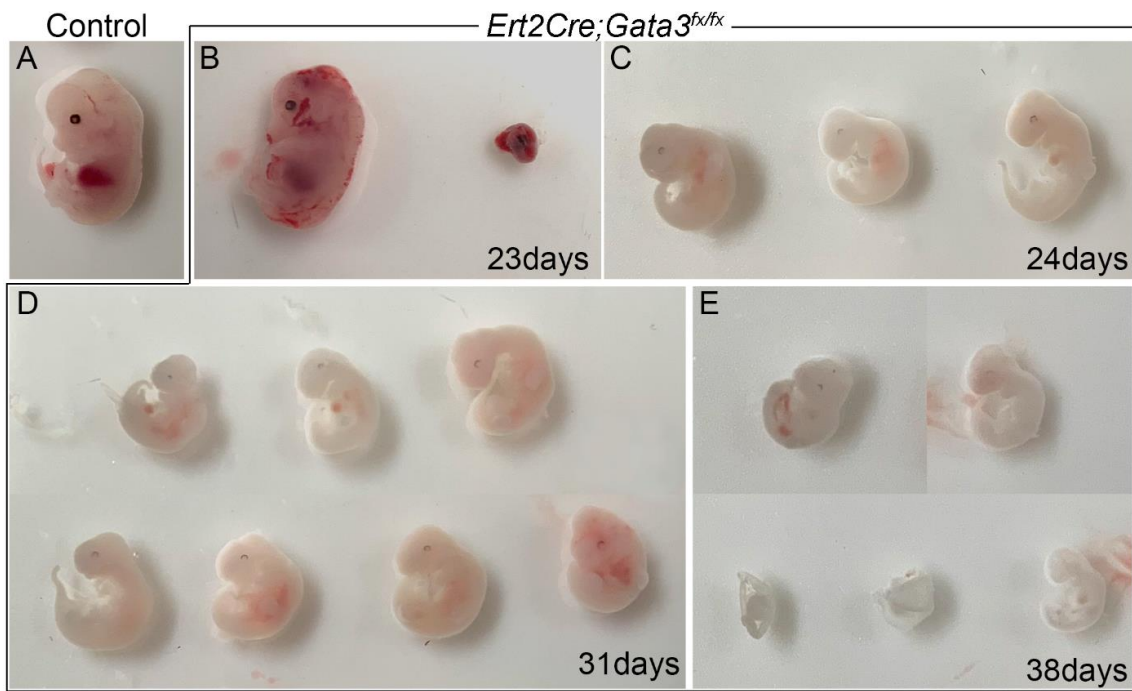


Figure.6.

374

375 **Figure 6. Retinoid-deficient diet in *Ert2Cre;Gata3<sup>f/fx</sup>* embryos resulted in increased early**

376 **lethality.** (A) E13.0 control embryo with retinoid-deficient food for 38 days. (B-E)

377 *Ert2Cre;Gata3<sup>f/fx</sup>* embryos whose mother was fed retinoid-deficient food before fertilization. The

378 days indicated in each figure show the duration of retinoid-deficient diet.

379

Table.1 Variation of the phenotype in present study

	Choanal Deformation ( CA + CS )	Lethal	CD + Lethal	
<i>Gata3<sup>fx/fx</sup></i>	0% ( 0/50 )	4% ( 2/50 )	4% ( 2/50 )	}
<i>Ert2Cre;Gata3<sup>fx/fx</sup></i>	31% ( 11/35 )	34% ( 12/35 )	66% ( 23/35 )	
Vitamin A deficient <i>Gata3<sup>fx/fx</sup></i>	0% ( 0/14 )	7% ( 1/14 )	7% ( 1/14 )	}
Vitamin A deficient <i>Ert2Cre;Gata3<sup>fx/fx</sup></i>	6% ( 1/17 )	94% ( 16/17 )	100% ( 17/17 )	

CA, Choanal Atrasia; CS, Choanal Stenosis; CD, Choanal Deformation \* : p<0.05

Table.1.

380

381

382       **References**

383

- 384       1           Trainor, P.A. and Andrews, B.T. (2013) Facial dysostoses: Etiology, pathogenesis and  
385 management. *Am J Med Genet C Semin Med Genet*, **163C**, 283-294.
- 386       2           Dixon, M.J., Marazita, M.L., Beaty, T.H. and Murray, J.C. (2011) Cleft lip and palate:  
387 understanding genetic and environmental influences. *Nat Rev Genet*, **12**, 167-178.
- 388       3           Kurosaka, H. (2019) Choanal atresia and stenosis: Development and diseases of the nasal  
389 cavity. *Wiley Interdiscip Rev Dev Biol*, **8**, e336.
- 390       4           Kurosaka, H., Wang, Q., Sandell, L., Yamashiro, T. and Trainor, P.A. (2017) Rdh10 loss-of-  
391 function and perturbed retinoid signaling underlies the etiology of choanal atresia. *Hum Mol Genet*, in  
392 press.
- 393       5           Kwong, K.M. (2015) Current Updates on Choanal Atresia. *Front Pediatr*, **3**, 52.
- 394       6           Lesciotto, K.M., Heuze, Y., Jabs, E.W., Bernstein, J.M. and Richtsmeier, J.T. (2018) Choanal  
395 Atresia and Craniosynostosis: Development and Disease. *Plast Reconstr Surg*, **141**, 156-168.
- 396       7           Dupé, V., Matt, N., Garnier, J.M., Chambon, P., Mark, M. and Ghyselinck, N.B. (2003) A  
397 newborn lethal defect due to inactivation of retinaldehyde dehydrogenase type 3 is prevented by maternal  
398 retinoic acid treatment. *Proc Natl Acad Sci U S A*, **100**, 14036-14041.
- 399       8           Barakat, A.J., Raygada, M. and Rennert, O.M. (2018) Barakat syndrome revisited. *Am J Med*  
400 *Genet A*, **176**, 1341-1348.
- 401       9           Barakat, A.Y., D'Albora, J.B., Martin, M.M. and Jose, P.A. (1977) Familial nephrosis, nerve  
402 deafness, and hypoparathyroidism. *J Pediatr*, **91**, 61-64.
- 403       10          Van Esch, H., Groenen, P., Nesbit, M.A., Schuffenhauer, S., Lichtner, P., Vanderlinden, G.,  
404 Harding, B., Beetz, R., Bilous, R.W., Holdaway, I. *et al.* (2000) GATA3 haplo-insufficiency causes human  
405 HDR syndrome. *Nature*, **406**, 419-422.
- 406       11          Grigorieva, I.V., Mirczuk, S., Gaynor, K.U., Nesbit, M.A., Grigorieva, E.F., Wei, Q., Ali, A.,  
407 Fairclough, R.J., Stacey, J.M., Stechman, M.J. *et al.* (2010) Gata3-deficient mice develop parathyroid  
408 abnormalities due to dysregulation of the parathyroid-specific transcription factor Gcm2. *J Clin Invest*,  
409 **120**, 2144-2155.
- 410       12          Duncan, J.S. and Fritsch, B. (2013) Continued expression of GATA3 is necessary for cochlear  
411 neurosensory development. *PLoS One*, **8**, e62046.
- 412       13          Duncan, J.S., Lim, K.C., Engel, J.D. and Fritsch, B. (2011) Limited inner ear morphogenesis  
413 and neurosensory development are possible in the absence of GATA3. *Int J Dev Biol*, **55**, 297-303.
- 414       14          Grote, D., Souabni, A., Busslinger, M. and Bouchard, M. (2006) Pax 2/8-regulated Gata 3  
415 expression is necessary for morphogenesis and guidance of the nephric duct in the developing kidney.

416 *Development*, **133**, 53-61.

417 15 Zhu, J., Min, B., Hu-Li, J., Watson, C.J., Grinberg, A., Wang, Q., Killeen, N., Urban, J.F., Jr.,  
418 Guo, L. and Paul, W.E. (2004) Conditional deletion of Gata3 shows its essential function in T(H)1-T(H)2  
419 responses. *Nat Immunol*, **5**, 1157-1165.

420 16 Furusawa, J., Moro, K., Motomura, Y., Okamoto, K., Zhu, J., Takayanagi, H., Kubo, M. and  
421 Koyasu, S. (2013) Critical role of p38 and GATA3 in natural helper cell function. *J Immunol*, **191**, 1818-  
422 1826.

423 17 Metzler, M.A. and Sandell, L.L. (2016) Enzymatic Metabolism of Vitamin A in Developing  
424 Vertebrate Embryos. *Nutrients*, **8**.

425 18 Shannon, S.R., Moise, A.R. and Trainor, P.A. (2017) New insights and changing paradigms in  
426 the regulation of vitamin A metabolism in development. *Wiley Interdiscip Rev Dev Biol*, in press.

427 19 Sandell, L.L., Sanderson, B.W., Moiseyev, G., Johnson, T., Mushegian, A., Young, K., Rey,  
428 J.P., Ma, J.X., Staehling-Hampton, K. and Trainor, P.A. (2007) RDH10 is essential for synthesis of  
429 embryonic retinoic acid and is required for limb, craniofacial, and organ development. *Genes Dev*, **21**,  
430 1113-1124.

431 20 Sandell, L.L., Lynn, M.L., Inman, K.E., McDowell, W. and Trainor, P.A. (2012) RDH10  
432 oxidation of Vitamin A is a critical control step in synthesis of retinoic acid during mouse embryogenesis.  
433 *PLoS One*, **7**, e30698.

434 21 Pandolfi, P.P., Roth, M.E., Karis, A., Leonard, M.W., Dzierzak, E., Grosveld, F.G., Engel, J.D.  
435 and Lindenbaum, M.H. (1995) Targeted disruption of the GATA3 gene causes severe abnormalities in the  
436 nervous system and in fetal liver haematopoiesis. *Nat Genet*, **11**, 40-44.

437 22 Ruest, L.B., Xiang, X., Lim, K.C., Levi, G. and Clouthier, D.E. (2004) Endothelin-A receptor-  
438 dependent and -independent signaling pathways in establishing mandibular identity. *Development*, **131**,  
439 4413-4423.

440 23 Lemos, M.C. and Thakker, R.V. (2020) Hypoparathyroidism, deafness, and renal dysplasia  
441 syndrome: 20 Years after the identification of the first GATA3 mutations. *Hum Mutat*, **41**, 1341-1350.

442 24 Bonilla-Claudio, M., Wang, J., Bai, Y., Klysik, E., Selever, J. and Martin, J.F. (2012) Bmp  
443 signaling regulates a dose-dependent transcriptional program to control facial skeletal development.  
444 *Development*, **139**, 709-719.

445 25 Zwicker, D., Ostilla-Monico, R., Lieberman, D.E. and Brenner, M.P. (2018) Physical and  
446 geometric constraints shape the labyrinth-like nasal cavity. *Proc Natl Acad Sci U S A*, **115**, 2936-2941.

447 26 Kawauchi, S., Shou, J., Santos, R., Hébert, J.M., McConnell, S.K., Mason, I. and Calof, A.L.  
448 (2005) Fgf8 expression defines a morphogenetic center required for olfactory neurogenesis and nasal  
449 cavity development in the mouse. *Development*, **132**, 5211-5223.

450 27 Varner, V.D. and Nelson, C.M. (2014) Cellular and physical mechanisms of branching  
451 morphogenesis. *Development*, **141**, 2750-2759.

452 28 Kouros-Mehr, H., Slorach, E.M., Sternlicht, M.D. and Werb, Z. (2006) GATA-3 maintains the  
453 differentiation of the luminal cell fate in the mammary gland. *Cell*, **127**, 1041-1055.

454 29 Chia, I., Grote, D., Marcotte, M., Batourina, E., Mendelsohn, C. and Bouchard, M. (2011)  
455 Nephric duct insertion is a crucial step in urinary tract maturation that is regulated by a Gata3-Raldh2-Ret  
456 molecular network in mice. *Development*, **138**, 2089-2097.

457 30 Razick, S., Magklaras, G. and Donaldson, I.M. (2008) iRefIndex: a consolidated protein  
458 interaction database with provenance. *BMC Bioinformatics*, **9**, 405.

459 31 Shannon, P., Markiel, A., Ozier, O., Baliga, N.S., Wang, J.T., Ramage, D., Amin, N.,  
460 Schwikowski, B. and Ideker, T. (2003) Cytoscape: a software environment for integrated models of  
461 biomolecular interaction networks. *Genome Res*, **13**, 2498-2504.

462 32 Nagy, A. (2003) *Manipulating the mouse embryo : a laboratory manual*. Cold Spring Harbor  
463 Laboratory Press, Cold Spring Harbor, N.Y.

464 33 Sandell, L.L., Kurosaka, H. and Trainor, P.A. (2012) Whole mount nuclear fluorescent  
465 imaging: convenient documentation of embryo morphology. *Genesis*, **50**, 844-850.

466